

## APPLICATION OF COMPUTATIONAL MODELING TO THE KINETICS OF PRECIPITATION OF ALUMINUM NITRIDE IN STEELS

A. Costa e Silva<sup>a</sup>, L. Nakamura<sup>b</sup>, F. Rizzo<sup>c</sup>

<sup>a</sup> EEIMVR-UFF, Volta Redonda, RJ – Brasil

<sup>b</sup> Research Centre - Aperam, Timóteo, MG, Brasil

<sup>c</sup> DEMa-PUC RJ, Rio de Janeiro, RJ – Brasil

(Received 03 July 2012; accepted 30 October 2012)

### Abstract

In previous works the possibilities and limitations of the application of calculations in the Al-Fe-N system to describe the precipitation of AlN in steel, both in the solid state and during the solidification were discussed and some difficulties related to the extension of these calculations to more complex steel systems, due to limitations in the thermodynamic data were also presented.

Presently, the precipitation kinetics of AlN in ferrite (BCC) and austenite (FCC) is discussed. The correct description of the precipitation of AlN in both phases is relevant to: (a) the precipitation at higher temperatures, in the austenite field, that occurs in some steels, (b) the concurrent precipitation of this nitride with the annealing treatment, when the steel is mostly ferritic, used in the processing of some types of deep drawing steels (c) the precipitation of this nitride in some silicon alloyed electric steels at relatively high temperatures, when these steels can have significant fractions of BCC and FCC in their microstructure. The precise knowledge of the precipitation-dissolution behavior of AlN in special in these two latter classes of steels is of great importance to their correct processing. In this work, a computational tool for simulating multi-particle precipitation kinetics of diffusion-controlled processes in multi-component and multi-phase alloy systems is employed in an attempt to describe these precipitation processes. The results are compared with experimental data on precipitation. The assumptions necessary for the application of the multi-particle modeling tool are discussed, agreements and discrepancies are identified and some possible reasons for these are indicated. Furthermore, the impact of the use of different sources of data on steel processing development is discussed and the need for further studies highlighted.

**Keywords:** computational thermodynamics, kinetic modeling, steel, AlN, PRISMA

### 1. Introduction

Aluminum nitride plays an important role in the processing of several steels (e.g. [1]). These include the control of the austenitic grain size during heat treatment and hot work as well as controlling or influencing texture in aluminum killed formable steel and effecting grain size and other properties in high silicon steels. Excess aluminum nitride, during solidification can be a cause of embrittlement of steel. In all these applications and cases, the control of the amount of nitride present in the different stages of processing is of paramount importance.

In previous works the thermodynamic aspects of the precipitation of AlN have been explored and discussed in relation to relevant applications [2,3]. This was of importance to establish the basis for any attempt at modeling the kinetics of precipitation and dissolution of this compound in steels. The series of

publications by Kozerschnik and co-workers [4,5,6] has marked a significant advance in the modeling of this precipitation reaction in steel. Furthermore, the availability of a computational tool for simulating multi-particle precipitation kinetics of diffusion-controlled processes in multi-component and multi-phase alloy systems [7] has stimulated an effort to evaluate the possibility of describing the precipitation kinetics of this compound in a reasonably accessible way.

### 2. Nucleation and Growth Precipitation Kinetics

Based on Langer-Schwartz theory [8] a commercial software (PRISMA) [7] that applies numerical methods to simulate the nucleation, growth and coarsening of precipitates that occur simultaneously in multi-component, multiphase

---

\* Corresponding author: andre@metal.eeimvr.uff.br

alloys was developed. All calculation in the present work employed this software. Although there are several important details in the implementation and the mathematical method used to tackle this problem on a “solvable” way, the fundamentals of the problem do not significantly differ from the classical theory related to the above mentioned phenomena (e.g. [9]). It is relevant to note, however, that by using these methods, PRISMA does not address individual particles, but is able to provide not only time dependent volume fraction information but also meaningful information on particle size distribution and number density, for instance. This is an important complementary tool in the toolbox of Integrated Computational Materials Engineering (ICME), since together, for instance, with DICTRA, that can provide one-dimensional diffusional growth information, or with phase-field methods, which normally focuses on a single or few precipitates with their morphologies, it will help better understand and quantify the several aspects of phase transformations.

Thus, while transport (during growth) is mainly treated as a diffusion problem, nucleation involves the effects of interfacial energy and, in the case of heterogeneous nucleation, the effect of microstructural features such as grain boundaries, junctions, etc. as well as dislocations. Furthermore, coarsening is highly influenced by interfacial energy.

It is thus evident that not only thermodynamic properties and atomic mobilities are needed to properly simulate these phenomena, but a complete set of new parameters, more or less accessible to measurement will be needed (interfacial energies ( $\sigma$ ), microstructural features and dislocation densities, mostly) if an adequate simulation is to be achieved. Furthermore, some parameters, as the interfacial energy have a very large effect on the overall results, influencing at the same time nucleation (the free energy of formation of a critical nucleus, for instance, depends on  $\sigma^3$ , while curvature chemical potential and critical radius are directly proportional to  $\sigma$ ).

When considering the need for this information, it is important to recall that other methods in ICME such as sharp interface, diffusional modeling with

DICTRA can also incorporate nucleation barriers and interfacial energy contributions, if this data is available [10]. Furthermore, like PRISMA, phase-field codes also do not provide any inherent nucleation model and need information on interfacial properties [11]. Coupling these different techniques could be very effective in bridging the modeling scales.

In the following section, a sensitivity analysis is performed for reasonable conditions for a basic steel, in order to clarify the importance of these parameters. For this analysis a deep drawing low carbon steel with 0.05%Al, 0.005%N and 0.3%Mn was selected. The thermodynamic data used was from TCFE7 database [12], whereas the mobilities were from MOBFE2 database [13]. Calculations involving the precipitation of AlN in austenite are centered on a grain size of 200 $\mu$ m, a reasonable estimate [14] for the temperatures used for completely dissolving the nitride, usually mentioned in the literature. In all cases the effect of hot working was not considered—i.e. dislocation densities compatible with recrystallized austenite ( $10^{10}$ - $10^{11}$  m $^{-2}$ ) were used. In this work this is referred to as the “model steel”. Hot work is known to have a dramatic effect on the precipitation kinetics of AlN (e.g. [15]). The values of interfacial energy are discussed in the next section.

## 2.1 Interfacial Energy

Kozeschnik and co-workers (e.g. [16]) stressed the importance of the values of interfacial energies and presented the calculation method for  $\sigma$  employed in their modeling effort. Unfortunately, information on the values used in their AlN in steel simulations was not directly available [5].

Table 1. Presents some values that can be found in the literature.

Furthermore, albeit there is no specific study for the interfacial energies of AlN in steel it is reasonable to expect this property to vary with temperature, as observed for  $M_{23}C_6$  in steel [23]. Finally, AlN can form in more than one crystal structure and in different morphologies, with variable coherency with

**Table 1.** Values of interfacial energy ( $\sigma$ ) between AlN and iron (steel)

Energy ( $\sigma$ ) (Jm $^{-2}$ )	Remarks	Source
1.56	Calculated: No information concerning crystal structures is given.	[17]
0.28	In BCC iron	[18]
0.1	In FCC iron (obtained by adjustment of model to data of [19])	[6]
0.75	In FCC iron (used by [19]. Value was derived by [20] for microalloy carbonitrides in FCC, not for AlN	[20,21]
1.4 to 2.7	Incoherent interface in BCC	[22]
0.5	Upper bound for a coherent interface with BCC	[22]
0.2	Upper bound for a coherent interface	[9]

the steel matrix (e.g. [24]): this should further complicate the evaluation of the interfacial energies.

Figure 1 shows the effect of the interfacial energy on the kinetics of precipitation of AlN in the “model steel” at 1000°C. As expected, there is a pronounced effect of interfacial energies in the nucleation of AlN in austenite.

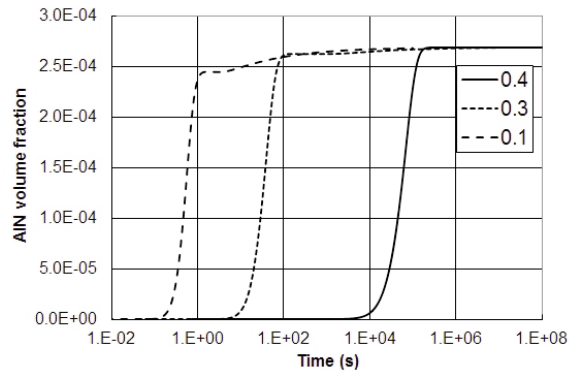


**Figure 1.** Calculated precipitated fraction of AlN in austenite at 1000°C for different values of interfacial energies ( $\sigma$ ) in  $Jm^{-2}$ , using the software PRISMA [7].

## 2.2 Matrix grain size and dislocation density

In the present work, for modeling purposes, heterogeneous nucleation was considered the operating nucleation mechanism. The sites considered were grain boundaries and dislocations. The first version of PRISMA [7], used in this work, calculates the density of nucleation sites based on a tetrakaidecahedron approximation of grains. With an aspect ratio of 1 the results are the same as those obtained by Cahn [25]. Nucleation at dislocations is calculated in a similar way. If one wants to consider

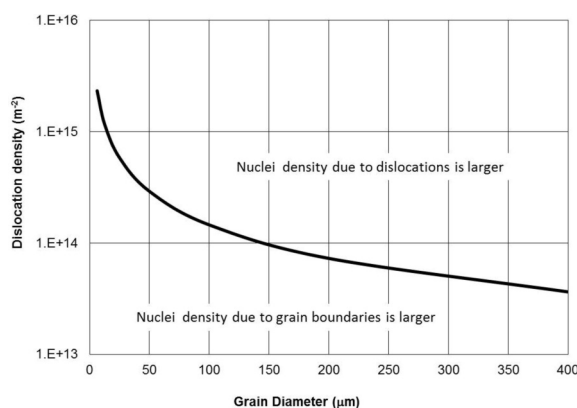


**Figure 2.** Conditions for equal densities of nuclei and for the predominance of nuclei in grain boundaries or at dislocations, in austenite (see text for discussion).

various nucleation sites, their densities can be calculated and then summed. Thus, one can define under which conditions which type of nucleation site will dominate, in the model. Figure 2 shows that in austenite treated at, say 1250-1300°C, for solubilization of AlN, with an expected grain sizes in the 100-200  $\mu m$  range, together with a recrystallized structure ( $\rho \approx 10^{11} m^{-2}$ ), grain boundary nucleation should be much more relevant than nucleation at dislocations, if the heterogeneous nuclei density is the dominating aspect.

Figure 3 presents the effect of varying the grain size on the kinetics of AlN precipitation in the “model steel”, at 1000°C with a fixed  $\sigma = 0.3 Jm^{-2}$ . Comparing these results with those presented in Figure 1 it is clear the effect of varying grain size is much smaller than that of varying the interfacial energy.

It is thus evident that, apart from the thermodynamic and mobility data, there are at least three relevant parameters to determine the kinetics of aluminum nitride precipitation: interfacial energy, by far the most important, and grain size and dislocation density.

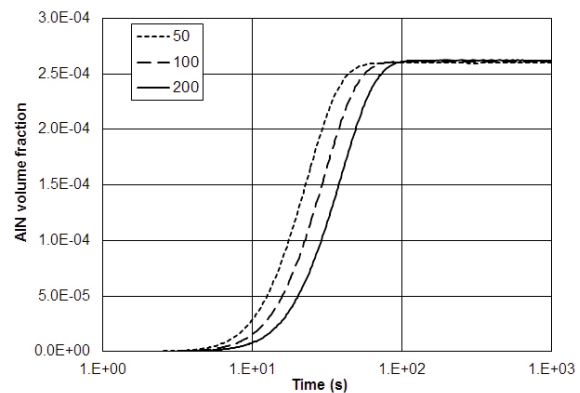


**Figure 3.** The influence of grain size on the precipitation of AlN in the “model steel”. Nuclei density calculated based on grain size. See text for discussion.

## 3. Application to selected data

### 3.1 Precipitation in ferrite in carbon steels

By far the most extensive volume of kinetic data for the precipitation of AlN in steels is for a matrix of ferrite (BCC) at temperatures under 800°C. The data of Borrelly and co-workers, in particular, who used careful TEP (thermoelectric power) measurements to follow the precipitation, appears to be reliable [26,27]. The results of the precipitation kinetics in an alloy containing 10ppm C, 10ppm Mn, 0.046%Al, 74ppm N and 49ppm O were used for comparison with the model. In the first stage, the value of  $\sigma$  was

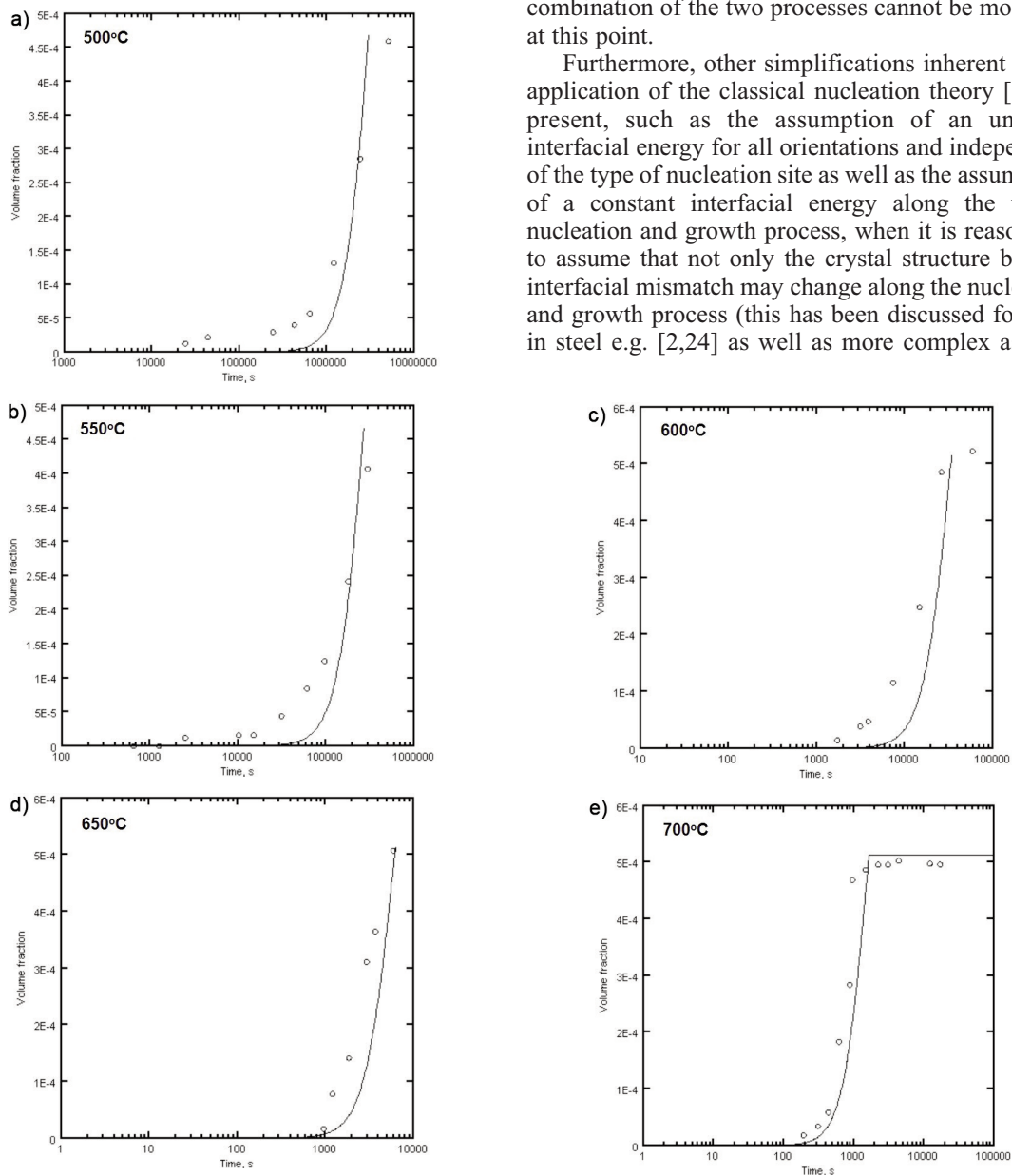
adjusted to the data. A value of  $\sigma=0.8\text{Jm}^{-2}$  was determined to result in a reasonable fit. Based on the processing cycle described by the authors and on the absence of explicit data, an ASTM grain size close to 9 ( $15\ \mu\text{m}$ ) and a  $\rho\cong 10^{12}\text{m}^{-2}$  were assumed to be reasonable for the ferrite before AlN precipitation annealing.

Figure 4 compares the results of Borrelly [26,27] with the values obtained in the present simulation for different annealing temperatures.

Although there is a general overall agreement some important discrepancies are noticed. In the

initial stages of precipitation the calculated curves deviate from the experimental data, for some temperatures. The model seems to underestimate the initial kinetics when compared to the data. Considering that the data is correct, this underestimation could be due to at least two simplifications in the present model. The effect of grain boundary diffusion superimposed on bulk diffusion is not considered. In the present model a single mobility is used: this can either describe bulk diffusion (as was done in the present case) or can describe grain boundary diffusion, if an “enhancement” factor is introduced. But the combination of the two processes cannot be modeled, at this point.

Furthermore, other simplifications inherent to the application of the classical nucleation theory [9] are present, such as the assumption of a uniform interfacial energy for all orientations and independent of the type of nucleation site as well as the assumption of a constant interfacial energy along the whole nucleation and growth process, when it is reasonable to assume that not only the crystal structure but the interfacial mismatch may change along the nucleation and growth process (this has been discussed for AlN in steel e.g. [2,24] as well as more complex aspects



**Figure 4.** (a) to (e). Calculated volume fraction of AlN precipitated in ferrite for different annealing temperatures. Experimental data from steel 1 in ref. [26]. Simulation performed with  $\sigma=0.8\text{Jm}^{-2}$  and grain size  $15\ \mu\text{m}$ .

such as, for instance, the presence of dislocation loops that might influence nucleation [28].

Within these limitations, however, the results are considered useful for the analysis of the precipitation kinetics of AlN in ferrite.

### 3.2 Precipitation in Austenite in carbon steels

Most of the experimental data on the kinetics of AlN precipitation in austenite is rather old. Furthermore, there are considerable experimental difficulties in performing these measurements at high temperatures. Some authors rely on the Beeghly's, method [29] involving sample dissolution followed by filtering of the particles: the accuracy of this method is questioned because of its potential lack of sensitivity when very fine precipitates are present [1,2]. Others rely only on measurements of soluble nitrogen to calculate the amount of nitride precipitated. On the other hand, Radis and co-workers [4] superimposed on their calculated TTT curve points indicating the presence or absence of AlN, after TEM observation.

A compilation of TTT information on the precipitation of AlN in austenite is presented in Figure 5. It must be noted that the data on this figure was obtained with steels of different compositions which influences the kinetics of precipitation, in special the driving force for precipitation.

The same procedure used to model the precipitation of AlN in ferrite was repeated in the case of an austenitic matrix. Individual isothermal experiments could be reasonably reproduced as indicated in Figure 6.

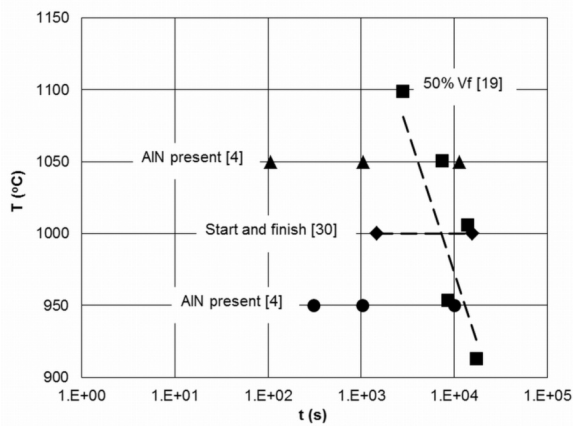


**Figure 5.** Compilation of TTT information on precipitation of AlN in annealed austenite. Radis and coworkers [4] (experiments where AlN was observed in TEM) Meyrhofer [19] (50% vf precipitated) (similar steels, with around 0.12%Al and 57ppm N) and Vodopivec [30] (experimental, start and finish of precipitation, steel with around 0.05%Al and 50ppm N).

In contrast with the case for a ferritic matrix, however, there was no single value of  $\sigma$ , independent of temperature, that could describe reasonably well the behavior of the precipitation of AlN in austenite, at different temperatures.

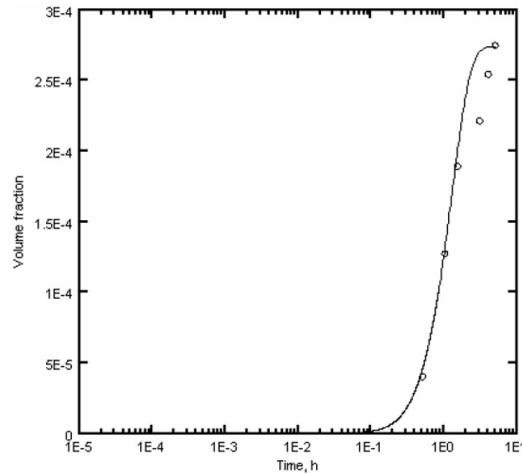


**Figure 6.** Precipitation kinetics in austenite in a steel with 0.12%Al and 57ppm N at 1100°C compared with experimental values of Mayrhofer [19]. Simulation used  $\gamma=0.36\text{Jm}^{-2}$  and a grain size of 200  $\mu\text{m}$ .

#### 3.2.1 Temperature variation of interfacial energy

A first attempt was made at varying the values of the interfacial energy with temperature. Using the results derived from two different C-Mn steels, namely the data of Meyerhoffer (19) at 1100°C and the results derived from the data of Vodopivec [30] at 1000°C, a value of  $\frac{d\sigma}{dT} = -0.75\text{mJm}^{-2}\text{K}^{-1}$  was obtained, which is in the same

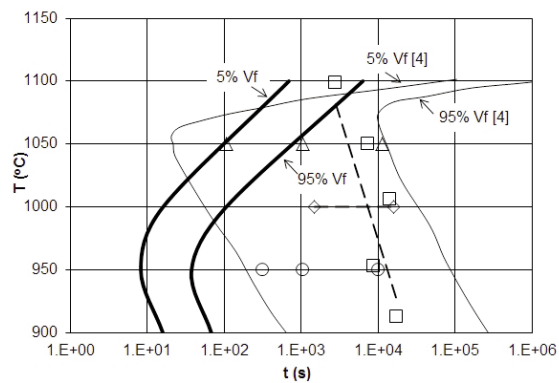


**Figure 7.** Calculated TTT diagram (bold lines, start at 5%  $V_f$  and end at 95%  $V_f$ ) for a steel with 0.12%Al and 57ppm N using a simple temperature variation model for the interfacial energy, compared with the collected information on the kinetics of AlN precipitation in austenite and the TTT curve of [4] (fine lines).

order of magnitude of the values reported by Murr [23] for  $M_{23}C_6$  in austenite. Figure 7 presents the results of the first attempt at reproducing the TTT behavior of the precipitation in austenite. The comparison with the previous collection of data (Figure 5) shows that the adjustment is still not very good, probably due to the use of data from two completely different steel compositions, with respect to Al and N contents.

#### 4. Conclusions and further work

Classical modeling of precipitation kinetics of AlN in steel is strongly dependant on interfacial energy ( $\sigma$ ). The adjustment of the model in the ferrite region is subjected to some limitations but the results are considered useful for the analysis of the precipitation kinetics of AlN in ferrite. While it seems possible to adjust a single parameter for  $\sigma$  to describe the precipitation in ferrite at low temperatures the same does not appear to be possible for the precipitation at high temperature in austenite. The scarcity of good experimental data in these high temperature conditions further complicates the attempts at finding good adjustment of the model, even when attempting to describe  $\sigma$  as a linear function of temperature. The current model uses a lumped density of heterogeneous nuclei so it is not possible to discuss, for instance TEM observations related to preferential precipitation sites, such as presented in [24]. If the modeling is to have a reduced number of adjustable parameters, new interfacial energy measurements or calculations are needed [16, 31]. In special the accurate modeling of AlN in high silicon steels, when both austenite and ferrite are present at high temperatures will depend on the ability to properly determine these values.

In the next stage of the work better descriptions of the kinetics of the precipitation in austenite will be attempted through the improvement of the adjustment of the interfacial energies and an attempt to extrapolate the interfacial energy in ferrite will be made.

#### Acknowledgements

ACS and FR thank CNPq and FAPERJ for their support; ACS thanks B. Böttger, Q. Chen, B. Hallstedt, E. Kozeschnik and B.-J. Lee for discussions and help during the course of this work.

#### References

- [1] F.G. Wilson, T. Gladman, International Materials Review, 33(5) (1988) 221–288.
- [2] A. Costa e Silva, F. Rizzo, J.G. Speer, Abstract and Programm Book CALPHAD XXX, York, England, 2001, p.106.
- [3] A. Costa e Silva, M.A. da Cunha, L. Nakamura, F. Rizzo, Abstract and Programm Book CALPHAD XL, Rio de Janeiro, Brasil, 2011, p. 170.
- [4] R. Radis, S. Schwarz, S. Zamberger, E. Kozeschnik, Steel Research International. 82(8) (2011) 905–910.
- [5] R. Radis, E. Kozeschnik, Modelling Simul. Mater. Sci. Eng., 18 (5) (2010) 055003.
- [6] E. Kozeschnik, V. Pletenev, N. Zolotarevsky, B. Buchmayr, Metallurgical and materials transactions A. 30(6) (1999) 1663–1673.
- [7] TCAB, TC-PRISMA, Manual and user's guide, version 1.0, TCAB, Stockholm, Sweden, 2011.
- [8] J. Langer, A. Schwartz. Phys Rev A, 21 (1980) 948–958.
- [9] D.A. Porter, K.E. Easterling, Phase transformations in metals and alloys, 2nd. ed. Chapman & Hall, London, 1992.
- [10] TCAB, DICTRA User's Guide, version 26, TCAB, Stockholm, Sweden, 2010.
- [11] N. Moelans, B. Blanpain, P. Wollants, CALPHAD, 32 (2008) 268–294.
- [12] TCAB, TCFE7 Database, TCAB, Stockholm, Sweden, 2012.
- [13] TCAB, MOBFE2 Database, TCAB, Stockholm, Sweden, 2011.
- [14] I. Kozasu, Processing- Thermomechanical controlled processing. In: F.B. Pickering editor. Materials Science and Technology- Constitution and Properties of Steels. Wiley-VCH, New York, 1996.
- [15] J.P. Michel, J.J. Jonas, Acta Metallurgica. 29(3) (1981) 513–26.
- [16] B. Sonderegger, E. Kozeschnik, Metallurgical and Materials Transactions A, 40(3) (2009) 499–510.
- [17] O.Y. Kontsevoi, A.J. Freeman, J.W. Jerome, Quantum Engineering of 3D Interfaces. D-3-D Annual review meeting. 2008.
- [18] G.A. Duit, A. Hurkmans, J.J.F. Scheffer, T.M. Hoogendorn, Proc. "THERMEC" 88. Keidanren Kaikan, Tokyo, Japan, 1988, p.114–121.
- [19] M. Mayrhofer, Berg. Huettenmaenn. Monatsheft, 120 (1975) 312–21.
- [20] H. Zurob, Y. Brechet, G. Purdy, Acta Materialia, 49 (20) (2001) 4183–90.
- [21] Y. Kang, H. Yu, J. Fu, K. Wang, Z. Wang, Materials Science and Engineering: A, 351(1) (2003) 265–71.
- [22] M.H. Biglari, C.M. Brakman, E.J. Mittemeijer, S. Van Der Zwaag, Metallurgical and Materials transactions A. 26(4) (1995) 765–776.
- [23] L. Murr, G. Wong, R. Horylev, Acta Metallurgica, 21(5) (1973) 595–604.
- [24] M. Sennour, C. Esnouf, Acta Materialia, 51(4) (2003) 943–957.
- [25] J.W. Cahn, Acta Metallurgica, 4 (5) (1956) 449–459.
- [26] A. Brahmi, R. Borrelly, Acta Metallurgica, 45 (5) (1997) 1889–1897.
- [27] I. Biron, R. Borrelly, P. Deleneau, B.J. Thomas, Mem. Sci. Rev. Metallurgie, 88 (1991) 725–33.
- [28] E. Furubayashi, H. Endo, H. Yoshida. Materials Science and Engineering, 14 (1974) 123–130.
- [29] H.F. Beeghly, Anal. Chem., 21(12) (1949) 1513–1519.
- [30] F. Vodopivec, Journal Iron Steel Institute, 211 (1973) 664–665.
- [31] A. Costa e Silva, J. Agren, M.T. Clavaguera-Mora, D. Durojvic, T. Gomez-Acebo, B.-J. Lee, Z.K.-Liu, P. Miodownik, H.J. Seifert, CALPHAD, 31 (2007) 53–74.